

# Quantitative Glycopeptide Changes in Rat Sperm During Epididymal Transit<sup>1</sup>

Ana Izabel Silva Balbin Villaverde, Louise Hetherington, and Mark A. Baker<sup>2</sup>

Priority Research Centre in Reproductive Science, School of Environmental and Life Sciences, University of Newcastle, Callaghan, NSW, Australia

## ABSTRACT

Mammalian spermatozoa acquire fertilizing potential as they undergo a series of changes during epididymal transit. One major facet of such is the alterations in the sperm glycome. Modifications of the sialic acid content within glycan moieties are known to regulate epitope presentation and cellular adhesion and signaling, all of which may be critical for sperm to successfully reach and fertilize the egg. To date, there is paucity of information regarding the sialic acid changes that occur on spermatozoa during epididymal transit. Therefore, the aim of this study was to identify *N*-linked sialylated glycoproteins in rat epididymal sperm and investigate whether they are regulated during epididymal transit. Sialylated glycopeptides from caput, corpus, and cauda spermatozoa were enriched using titanium dioxide beads. Bound *N*-linked glycopeptides were released by enzymatic deglycosylation using PNGase F and then analyzed by liquid chromatography tandem-mass spectrometry. A total of 92 unique *N*-linked sialylated glycopeptides were identified from 65 different proteins. These included members of the disintegrin and metalloproteinase domain-containing protein family (ADAM), Basigin, and Testis-expressed protein 101 (TEX101). Remarkably, label-free quantification showed that more than half of these peptides (48/92) were regulated during epididymal transit. Of interest, the protein TEX101 exhibited PNGase F-resistant deglycosylation under the conditions used in this study. The results from this study showed that changes in the *N*-linked sialoglycoprotein profile is a major hallmark of sperm maturation in rats.

ADAM family, LC-MS/MS, sialic acid, TEX101, titanium dioxide

## INTRODUCTION

Glycosylation is one of the most common and important posttranslational modifications of proteins, in which oligosaccharide chains are covalently linked at either Serine/Threonine residues (*O*-linked) or Asparagine residues (*N*-linked). In the case of *N*-linked glycoproteins, the presence of a canonical peptide sequence (NXS/T, where X can be any amino acid except Proline) is essential for this type of glycosidic attachment to occur. Studies involving mutations, which

prevent the formation of specific glycoconjugates, have shown how diverse the roles of *N*-glycosylation can be [1, 2]. In this context, the carbohydrate composition is considered an important feature, determining the influence of glycosylation on proteins. For example, the presence of sialic acid (Sia), a negatively charged nine-carbon monosaccharide usually located at the end of glycan structures, is known to interfere with the physiochemical properties of proteins as well as to participate in the masking of cell-surface antigens or in specific recognition sites [3].

During migration from the proximal to the distal portion of the epididymis, sperm cells undergo a series of molecular and biochemical changes that are essential for the production of a functionally gamete [4, 5]. Notably, as spermatozoa transit through the epididymis, changes in sperm glycome have been demonstrated to occur by means of proteolytic processing [6, 7], shedding [8], or incorporation [9] of glycoproteins as well as by the rearrangement of the glycan moieties [10, 11]. The latter is likely to be a result of glycan-modifying enzymes (glycosyltransferases and glycohydrolases) mainly present in the luminal fluid of the epididymis, with a remnant located at the surface of spermatozoa [12, 13].

Comparison of either rabbit [14], ram [15], chimpanzee [16], or boar [17] spermatozoa has demonstrated an overall increase in their surface negative charge during epididymal transit. This observation has been suggested to be a result of an increase in the Sia content of spermatozoa. In agreement with this, the use of the lectin wheat germ agglutinin (WGA), which selectively binds to *N*-acetylglucosamine (GlcNAc) and Sia residues, shows an increase in labeling intensity of more mature epididymal spermatozoa [18–21]. In addition, treatment of mature sperm cells with neuraminidase to remove terminal Sia residues reduces WGA labeling in ram and human sperm [18, 22]. Thus, although sialyltransferase activity was found to be higher in the caput region of rat epididymis when compared to the cauda region [12, 23], clearly sialylation itself becomes accumulative during sperm transit.

Studies with murine, macaque, and chicken spermatozoa, in which surface Sia was removed by neuraminidase, have demonstrated the importance of this negative sugar for sperm to bypass the cervical mucus [9], colonize chicken sperm reservoirs [24], prevent phagocytosis by macrophages [25], protect surface epitopes from anti-sperm antibodies [26], and attach to oviductal epithelial cells [27]. Additionally, terminal Sia residues have been implicated in the protection of receptor(s) that are essential for oocyte binding. Consistent with this, human spermatozoa subjected to desialylation exhibit higher zona pellucida binding when compared to untreated samples [22]. Likewise, the addition of neuraminidase inhibitors during capacitation decreases the ability of mouse spermatozoa to bind to homologous zona pellucida [28].

Despite these findings, there is a lack of studies to identify maturation-related changes in the sialome of mammalian sperm. In this regard, a proteomic approach based on mass spectrometry (MS) is a valuable tool, allowing a large-scale

<sup>1</sup>This work was supported by the Brazilian National Council for Scientific and Technological Development (CNPq).

<sup>2</sup>Correspondence: Mark A. Baker, Priority Research Centre in Reproductive Science, School of Environmental and Life Sciences, University of Newcastle, Callaghan, New South Wales 2308, Australia.  
E-mail: Mark.Baker@newcastle.edu.au

Received: 5 August 2015.  
First decision: 20 September 2015.  
Accepted: 4 March 2016.

© 2016 by the Society for the Study of Reproduction, Inc. This article is available under a Creative Commons License 4.0 (Attribution-Non-Commercial), as described at <http://creativecommons.org/licenses/by-nc/4.0>

eISSN: 1529-7268 <http://www.biolreprod.org>  
ISSN: 0006-3363

analysis of the glycosylated proteins. However, due to the complexity and heterogeneity of glycans and the relatively low abundance of glycopeptides [29], techniques for the enrichment of these peptides are required before performing a MS analysis. Therefore, in the present study, titanium dioxide (TiO<sub>2</sub>) was used to enrich for Sia-containing glycopeptides followed by liquid chromatography tandem-mass spectrometry (LC-MS/MS) for their identification. Using this approach, sialylated N-glycoproteins present in rat spermatozoa from caput, corpus, and cauda epididymis were successfully identified and the glycosylation sites annotated. In addition, we performed a label-free quantification to investigate the regulation of these N-glycoproteins during epididymal transit in rats.

## MATERIALS AND METHODS

### Materials

Unless otherwise stated, chemicals were purchased from Sigma-Aldrich at the highest research grade available. Antarctic phosphatase and Peptide-N-Glycosidase F (PNGase F) were purchased from New England Biolabs. Trifluoroacetic acid (TFA), acetonitrile (ACN), and glycolic acid were from Fluka. D-Glucose was obtained from Australian Scientific. The bicinchoninic assay kit was from Quantum Scientific. Precast 4%–20% SDS gels were from NuSep Ltd. Percoll was supplied by GE Healthcare. HEPES was from Invitrogen Australia. Hams F10 was from MP Biomedical. Sequencing-grade trypsin was supplied by Promega. Protease inhibitor tablets Complete Mini was purchase from Roche Life Science. Chloroform was purchased from Fronine at the highest purity available. Glycine and Tris were from AMRESCO Life Science Research. The TiO<sub>2</sub> was collected from a disassembled column.

### Recovery of Spermatozoa

Animal use was approved by institutional and New South Wales State Government ethics committees. Adult Wistar rats (~8 to 10 wk old) were asphyxiated, perfused intracardially, and the epididymides were removed. Sperm cells were retrieved from the caudal region of the epididymides by retrograde flushing [30, 31]. After dispersion in 0.3% bovine serum albumin (BSA) Biggers-Whitten-Whittingham (BWW) media [32] for 10–15 min at 37°C, caudal sperm cells were washed three times (400 × g, 3 min) using BWW media without BSA to remove residual epididymal fluid. Caput and corpus regions of the epididymides were finely sliced using a surgical-grade scalpel, and sperm cells were gently teased out into 0.3% BSA BWW media. Spermatozoa were submitted to Percoll density separation (30%) to eliminate epithelial cell contamination [33] and then washed three times (400 × g, 3 min) with BWW media without BSA.

### Sperm Protein Extraction and Preparation

Sperm pellets were resuspended in a lysis buffer consisting of 1% (w/v) C7BzO (3-[4-heptyl] phenyl-3-hydroxypropyl)dimethylammoniopropanesulfonate), 7 M urea, 2 M thiourea, and 40 mM Tris (pH 10.4) at a final concentration of 2.5 × 10<sup>6</sup>/100 μl. Samples were incubated for 1 h at 4°C with constant rotation and the supernatant recovered after centrifugation (18 000 × g, 15 min, 4°C). Protein quantification was performed using a two-dimensional quantification kit (G.E. Healthcare) following the manufacturer's protocol. A total of 500 μg of protein for each sample was reduced and then alkylated using 10 mM dithiothreitol (DTT) and 45 mM iodoacetamide, respectively, with a 30 min incubation period at 30°C for each step. Protein was precipitated using methanol and chloroform [34], and the pellet was resuspended with trypsin in a buffer containing 25 mM ammonium bicarbonate and 1 M urea at 1:50 trypsin to protein ratio and then incubated overnight at 37°C with constant agitation. Proteases were inactivated using bath sonication, and peptide samples were treated with alkaline phosphatase (20 U) at 30°C for 2 h with constant shaking.

### Sialoglycopeptide Enrichment

Enrichment of glycopeptides containing terminal Sia was performed as previously described with slight modifications [35]. Peptide samples were dried to ~100 μl in a vacuum concentrator, diluted with 1 ml of loading buffer—1 M glycolic acid, 80% (v/v) ACN, 5% (v/v) TFA—and then applied to TiO<sub>2</sub> beads (2 mg) pre-equilibrated in 80% ACN. After a 1 h incubation period at room temperature with constant rotation, TiO<sub>2</sub> beads were washed twice with loading

buffer, twice with washing buffer 1 (80% [v/v] ACN, 1% [v/v] TFA), and once with washing buffer 2 (20% [v/v] ACN, 0.1% [v/v] TFA). Beads were dried by vacuum centrifugation for 5 min. Bound dephosphorylated sialoglycopeptides were then released from the beads by enzymatic deglycosylation treatment. In brief, dried TiO<sub>2</sub> beads were resuspended in 40 μl of 50 mM ammonium bicarbonate, and 1 μl of PNGase F was added. After incubation for 3 h at 37°C with constant agitation, deglycosylated peptides were recovered in the supernatant (17 000 × g, 5 min), and TiO<sub>2</sub> beads were washed once with 50 mM ammonium bicarbonate to enhance peptide recovery. Deglycosylated peptides were then dried in a SpeedVac and resuspended in 0.1% (v/v) TFA.

### Lectin Affinity Purification

Rat sperm lysates were obtained as described above. Approximately 50 μl of a 50% slurry of either WGA or *Sambucus nigra* (SNA) lectin was washed three times in 0.5 M NaCl, 20 mM Hepes, 1 mM CaCl<sub>2</sub>, 1 mM MgCl<sub>2</sub>, then added to 100 μg of sperm lysates. The mixture was left to incubate at 4°C for 1 h, after which the lectin beads were pelleted (400 × g, 1 min) and the supernatant removed. The beads were resuspended and subsequently washed in the same washing buffer. Elution of the protein was specific to the lectin. For WGA, we used 0.5 M GlcNAc, whereas for SNA, we used 0.1 M lactose in Tris-buffered saline followed by 0.1 M lactose in 0.2 M HCl.

### Mass Spectrometry

The resuspended peptides were loaded on LC-MS and run essentially as described previously [36].

### Bioinformatics

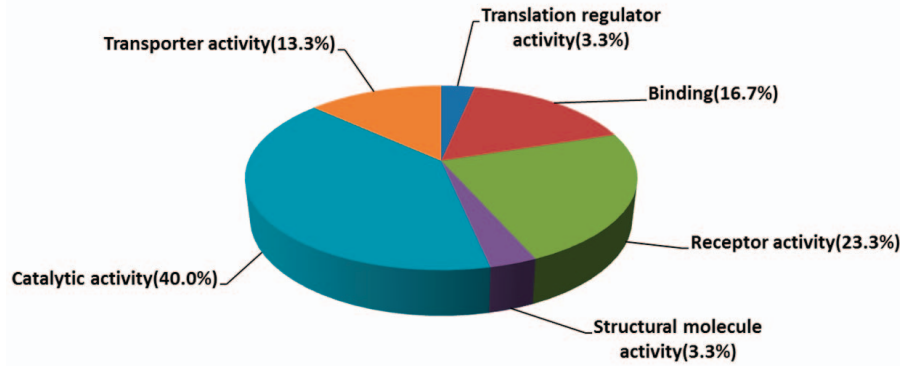
Acquired collision-induced dissociation spectra were processed in Data-Analysis 4.0; deconvoluted spectra were further analyzed with BioTools 3.2 software and submitted to Mascot database search (Mascot 2.2.04, Swissprot database: 546 439 sequences; 194 445 396 residues, release date 19/20/14). The species was set at *Rattus*, parent peptide mass tolerance ± 0.7 Da, fragment mass tolerance ± 1.2 Da, and enzyme specificity trypsin with two missed cleavages. The following variable modifications have been used: phosphorylation, carbamidomethylation, deamidation, and oxidation. To identify N-linked glycosylation sites, a deamidated Asparagine residue had to be flanked by the glycosylation consensus motif (NXS/T, where X is any amino acid besides Proline) that was manually validated. Peptides that were assigned a deamidation event based solely on the MS data (i.e., no y- or b- fragment ion for a particular deamidated Asparagine residue could be detected) were presumed to be glycosylated only if a canonical N-glycan motif was present.

The derived MS datasets on the three-dimensional trap system were combined into protein compilations using the ProteinExtractor functionality of Proteinscape 2.1.0 573 (Bruker Daltonics), which conserved the individual peptides and their scores while combining them to identify proteins with much higher significance than achievable using individual searches. In order to exclude false-positive identifications, peptides with Mascot scores below 40 were rejected. Peptides with a mascot score above 40 were initially accepted but then manually validated in BioTools (Bruker Daltonics) on a residue-by-residue basis using the raw data to ensure accuracy. In brief, the ion series were inspected to ensure that the peaks being selected were not simply baseline, the accuracy between the residues was less than 0.15 Da, and, preferentially, an overlapping ion series was found.

### Peptide Quantification and Statistical Analysis

MS-based label-free quantification of the N-glycopeptides identified was performed using the software Data Analysis 4.1 (Bruker Daltonics). Peptides were matched based on charge state, m/z value, and elution time. The match was confirmed by visual localization of the peptide on the survey view and by manual comparison of the MS/MS spectra if available. Relative peptide quantification was carried out by integrating the area of the extracted ion chromatograms of the monoisotopic peak from the MS spectra. Detection parameters were set at 99% sensitivity, intensity threshold of 10%, and minimum peak valley of 10%. The area under the monoisotopic peak (± 0.2 m/z) was recorded for each peptide. Peaks below the signal-to-noise ratio of 4 were assigned as having an area equal to zero. Overlapping peptides were not considered. Isotopic peaks other than the monoisotopic one were used for the same peptide in all runs when the area of the latter could not be accurately calculated. If oxidation of the peptide was additionally detected (often introduced during sample preparation), the integrated peptide intensity of both the oxidized and nonoxidized forms of the peptide were summed. Normalization of the data was achieved by using the average area of five

A



B

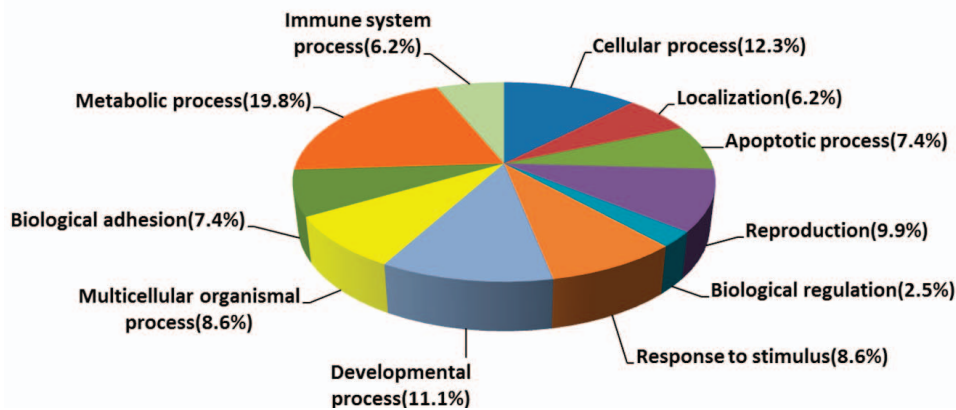


FIG. 1. Classification of sperm sialylated N-glycoproteins regulated during epididymal transit in rats based on their molecular function (A) and biological process properties (B).

different peptides visually selected based on the quality and constant intensity of the MS spectra among the samples. The data obtained for the three regions of the epididymis (caput vs. corpus vs. cauda) from four animals were compared using Student *t*-test. *P*-values < 0.05 were considered as significant.

### Enzymatic Deglycosylation of Proteins and Immunoblotting

Sperm cells from the caput, corpus, and caudal regions of the epididymis were lysed in 20 mM 3-[(3-cholamidopropyl)dimethylammonio]-1-propanesulfonate (CHAPS) and 25 mM Tris buffer (pH 7.0) for 1 h at 4°C with constant rotation. For testicular protein recovery, rat testis were sonicated using low frequency to disperse tissue in 0.5 M NaCl and 20 mM Tris buffer and cells were washed twice (18 000 × *g*, 15 min, 4°C). Pellets were resuspended in lysis buffer and incubated for 1 h at 4°C with constant rotation. Proteins from testicular tissue were also extracted from adult Swiss mice (~8 to 10 wk old) using the protocol described above. Following sperm recovery, rat epididymal tissue were macerated and then boiled for 5 min with a buffer consisting of 2% (w/v) SDS, 185 mM Tris, and protease inhibitors (pH 6.8). For ADAM7 blots, proteins from rat sperm cells were extracted similarly as described for epididymal tissue. Spermata containing sperm, testicular, or epididymal proteins were recovered after centrifugation (18 000 × *g*, 15 min, 4°C), and protein quantification was performed using the bicinchoninic method.

Protein samples were treated with the endoglycosidase PNGase F prior to immunoblotting. Briefly, a denaturing buffer was added to samples (12–40 μg of total protein) resulting in a final concentration of 0.5% (w/v) SDS and 50 mM DTT or 1% (v/v) 2-mercaptoethanol, and the proteins were boiled for 10 min. Samples were then supplemented with 50 mM sodium phosphate, 1% (v/v) NP-40, 1 mM ethylenediaminetetraacetic acid, and 385–770 U/ml PNGase F and incubated overnight at 37°C with constant agitation. Control samples were not supplemented with PNGase F.

After deglycosylation, proteins were precipitated using methanol and chloroform, resuspended in SDS-PAGE sample buffer, separated by SDS-

PAGE, and then transferred onto nitrocellulose membrane Watman Optitran BA-S 85 (GE Healthcare). Membranes were blocked with Tris-buffered saline with Tween-20 (TBS-T)—0.02 M Tris, 0.15 M NaCl, and 0.1% (v/v) Tween-20 (pH 7.6)—containing 5% (w/v) skim milk for 1 h at room temperature (Basigin and TEX101) or overnight at 4°C (ADAM7). The blots were then incubated overnight at 4°C with goat polyclonal antibody raised against TEX101 (S-13) (1:500 dilution; Santa Cruz Biotechnology Inc.), Basigin (G-19) (1:1000 dilution; Santa Cruz Biotechnology Inc.), or for 6 h with ADAM7 antibody (M-20) (1:200 dilution; Santa Cruz Biotechnology Inc.) in 5% (w/v) skim milk TBS-T. As a control, a blocking peptide specific to anti-ADAM7 (1:100 dilution; Santa Cruz Biotechnology Inc.), anti-TEX101 (1:250 dilution; Santa Cruz Biotechnology Inc.), and anti-Basigin (1:500 dilution; Santa Cruz Biotechnology Inc.) antibodies were used. The peptides were pre-incubated with primary antibody for 5 min before being added to the membrane. Membranes were washed three times for 5 min with TBS-T and then incubated for 1 h at room temperature with rabbit anti-goat immunoglobulin G (IgG) horseradish peroxidase conjugate (Santa Cruz Biotechnology Inc.) at a concentration of 1:1000 in 5% (w/v) skim milk TBS-T. After three washes as described above, immune-reacted proteins were detected using an enhanced chemiluminescence kit (Amersham International) according to the manufacturer's instructions.

### Immunocytochemistry

Intact sperm cells from testis and different regions of the epididymis (caput, corpus and cauda) were fixed in 4% (w/v) formaldehyde for 10 min at room temperature. Cells were washed three times in PBS containing 0.5 M glycine and then attached to poly-L-lysine coverslips. Spermatozoa were permeabilized with 0.2% (w/v) saponin in PBS for 10 min, washed, and blocked for 1 h with 3% (w/v) BSA in PBS. Coverslips were incubated overnight (4°C) with anti-TEX101 antibody or anti-Basigin antibody in a 1:50 dilution with PBS containing 1% (w/v) BSA, washed, and then incubated for 1 h with Alexa Fluor

TABLE 1. List of sialylated N-glycopeptides identified in rat sperm from different regions of the epididymis (caput, corpus, and cauda) and their regulation during epididymal transit.

Peptide	Lectin binding		Peptide sequence <sup>a</sup>	Fold change <sup>b</sup>		P value <sup>b</sup>		MS/MS <sup>c</sup>		
	SNA	WGA		Mascot score	Caput vs. corpus	Corpus vs. cauda	Caput vs. corpus		Corpus vs. cauda	
4F2 Cell-surface antigen heavy chain			K.LANASLYLAEWQNIITK.N *	64.7	1.47	1.18	1.73	0.185	0.056	1.1
5'-Nucleotidase precursor			K.VFEDDKGNVVTSYGNPILLNSTIR.E	56.8	-1.88	3.06	1.63	0.184	0.323	1.2
Alpha-1-inhibitor 3 precursor			K.YLNTEQQLTEK.I	66.3	ND	ND	ND	ND	ND	1.3
			K.EADNIFTSLLGPPVPEFWNK.S *	60.4	-2.04	-9.38	-19.16	0.186	0.111	1.4
			K.ELYESWQNFIDQK.L	47.8	ND	ND	ND	ND	ND	1.5
			K.TEDVSNFQNSTIK.R	80.7	-2.12	-1.54	-3.27	0.043	0.018	1.6
Angiotensin-converting enzyme			K.VLWNEYAEANWHYNTNIIIEGSK.I	66.3	-1.57	-1.67	-2.62	0.290	0.059	1.7
Acrosin precursor			R.VDLIDLDCNSTIQWYNGR.V	132.0	1.99	1.22	2.42	0.216	0.056	1.8
ADAM 18			K.EVNETGNDCAAK.K	69.6	-1.40	n/a	n/a	0.068	0.001	1.9
ADAM 1 precursor			R.NSLFCVGEPSDR.M	103.6	-1.09	n/a	n/a	0.272	0.007	1.10
			K.WICINGTCCSQAQCR.D	109.7	1.12	-10.76	-9.62	0.383	0.031	1.11
			R.GVLIQFNVSYGIEPLESSGFEHVYQVEPK.K	66.5	ND	ND	ND	ND	ND	1.12
ADAM 2 precursor			R.SFNSCMEDFSK.F	84.9	-4.49	-6.99	-31.35	0.045	0.034	1.13
			K.DNMSAAYGQIR.D	89.7	-1.12	-1.51	-1.69	0.371	0.015	1.14
ADAM 5			R.FLVDFOQCNIISR.D	65.8	-1.14	-1.14	-1.30	0.256	0.111	1.15
			K.APYATNYSCEGLNETIK.K	91.1	1.14	1.99	2.26	0.438	0.008	1.16
ADAM 7 precursor			R.EFLALNYSETYNIK.R	80.8	-2.15	6.48	3.02	0.092	0.003	1.17
A-kinase anchor protein 4 precursor			K.NOSLEFSAMK.A	50.5	1.67	1.53	1.09	0.458	0.058	1.18
Acid ceramidase			R.SVLENTSYEEAK.N	46.2	ND	ND	ND	ND	ND	1.19
			K.TQLTCLFNSSGIDIVGHR.W	80.0	-17.68	n/a	n/a	0.002	0.001	1.20
			K.TSDTGDQITISNGTEANSK.Y	93.6	1.38	-1.11	1.24	0.200	0.179	1.21
Basigin precursor			K.YVIISTPELSELIISDLDMNVDPGTYYVCNAINSQGSAR.E	100.5	ND	ND	ND	ND	ND	1.22
Calcium-binding and spermatid-specific protein 1			K.DAAEESVTNVTTEEPSVTSVVEQSGNKEDLSTNDSGIFK.L *	128.6	-1.25	-1.69	-2.11	0.239	0.071	1.23
Carboxypeptidase Q			K.EVMSLLQPLNIITK.V	58.0	-3.40	n/a	n/a	0.013	0.003	1.24
CD59 glycoprotein precursor			K.TNSICSPNLDACLVAVSGK.Q	94.3	1.07	2.91	3.11	0.376	0.004	1.25
CD63 antigen			K.DRVPDSCCINIYGCCNDPK.E	85.2	-1.28	1.37	1.07	0.235	0.332	1.26
			R.QELNIDSLQVAER.L	84.5	4.31	-6.46	-1.50	0.073	0.243	1.27
Clusterin precursor			R.QLEEFLLNQSSPFYFWMNGDR.I	69.7	n/a	n/a	n/a	0.050	n/a	1.28
Ciliary neurotrophic factor receptor alpha precursor			R.VNGIDLAPDLLNGSQLIIR.S *	72.9	-1.13	-4.24	-4.81	0.395	0.016	1.29
Cytochrome c oxidase subunit 4 isoform 1, mitochondrial precursor			R.IQFNESFAEMNK.G	63.8	1.27	-5.24	-4.13	0.242	0.017	1.30
Cation channel sperm-associated protein subunit delta			K.ANLIQFGNMYDGNK.F *	56.5	1.32	1.39	1.83	0.154	0.050	1.31
			K.LQDVNLHNFIR.G	50.3	-3.22	-16.03	-51.66	0.008	0.007	1.32
			R.HHFYTNISGLTSFGEK.V	93.7	-2.21	n/a	n/a	0.040	0.005	1.33
Dipeptidase 3 precursor			R.MCSAYPELELTSADG.LNSTQK.L	122.8	-3.39	-20.17	-68.36	0.012	0.012	1.34
			K.HNNDIQHIWESDSNEFSVIADPR.G *	86.0	-1.42	-2.50	-3.55	0.273	0.022	1.35
Endoplasmic reticulum chaperone protein alpha-4 precursor			R.EEAIQLDGLNASQIR.E	104.3	-1.69	-1.76	-2.97	0.029	0.036	1.36
Fibrinogen beta chain precursor			K.AINETAIVSMDDK.D	93.6	1.43	1.19	1.71	0.008	0.017	1.37
GDNF family receptor alpha-4 precursor			K.GTAGNALMEGASQLVGENRI.I *	59.4	-5.82	n/a	n/a	0.032	0.033	1.38
			R.AYAGLVGTVVTPNYLIDNVAR.V *	45.4	n/a	n/a	n/a	n/a	0.0004	1.39
Gamma-glutamyl hydrolase precursor			R.SINGVLLPGGGANLTHSGYSR.V	53.4	ND	ND	ND	ND	ND	1.40

GLYCOPEPTIDE CHANGES DURING RAT SPERM MATURATION

TABLE 1. Continued.

Peptide	Lectin binding		Peptide sequence <sup>a</sup>				Fold change <sup>b</sup>				P value <sup>b</sup>		MS/MS <sup>c</sup>
	SNA	WGA	Mascot score	Caput vs. corpus	Corpus vs. cauda	Caput vs. cauda	Corpus vs. cauda	Caput vs. corpus	Corpus vs. cauda	Caput vs. cauda	MS/MS <sup>c</sup>		
Gamma-glutamyl transpeptidase 1			67.8	n/a	n/a	1.32	0.010	0.019	0.255	1.41			
Beta-galactosidase-1-like protein 3			87.6	ND	ND	ND	ND	ND	ND	1.42			
GTP-binding protein 1	x		93.2	-2.21	-2.01	-4.45	0.005	0.113	0.005	1.43			
Solute carrier family 2, facilitated glucose transporter member 3			46.2	2.09	-1.13	1.85	0.042	0.301	0.125	1.44			
Beta-hexosaminidase alpha chain precursor	x		69.7	1.13	1.20	1.36	0.159	0.067	0.002	1.45			
Hexokinase-1		x	46.4	1.09	-1.30	-1.20	0.449	0.182	0.356	1.46			
Hyaluronidase PH-20 precursor		x	78.1	ND	ND	ND	ND	ND	ND	1.47			
Izumo sperm-egg fusion protein 1 precursor		x	54.0	ND	ND	ND	ND	ND	ND	1.48			
Casein kinase I isoform gamma-2		x	144.9	-3.29	1.51	-2.18	0.020	0.232	0.087	1.49			
Galectin-3-binding protein		x	97.7	-1.44	2.12	1.47	0.246	0.011	0.096	1.50			
Endothelial lipase precursor			109.7	1.02	1.55	1.58	0.486	0.189	0.149	1.51			
Lipid phosphate			101.6	1.06	-1.36	-1.29	0.333	0.055	0.072	1.52			
phosphohydrolase 1			89.2	1.93	-1.63	1.18	0.108	0.221	0.443	1.53			
Beta-mannosidase precursor			49.8	n/a	9.13	n/a	0.196	0.008	0.001	1.54			
Membrane cofactor protein precursor			86.2	1.48	4.08	6.03	0.369	0.021	0.002	1.55			
Sperm mitochondrial-associated cysteine-rich protein			75.9	n/a	7.29	n/a	0.196	0.006	0.010	1.56			
Membrane metallo-			74.4	n/a	n/a	n/a	n/a	0.001	0.001	1.57			
endopeptidase-like 1			108.1	1.03	2.02	2.07	0.458	0.021	0.051	1.58			
Nicastrin precursor			73.8	ND	ND	ND	ND	ND	ND	1.59			
Biglycan precursor			52.9	1.10	1.71	1.88	0.340	0.012	0.002	1.60			
Decorin precursor			78.7	-1.48	n/a	n/a	0.132	0.062	0.024	1.61			
Putative phospholipase B-like 2			121.9	1.57	-1.06	1.48	0.195	0.384	0.121	1.62			
Serine protease 40			103.4	1.43	-1.36	1.05	0.130	0.169	0.370	1.63			
Serine protease 46			87.8	1.30	-1.11	1.17	0.081	0.174	0.163	1.64			
Inactive serine protease 54			72.8	2.05	1.03	2.11	0.072	0.468	0.025	1.65			
Ammonium transporter Rh type C			66.5	-5.92	n/a	n/a	0.061	0.091	0.027	1.66			
RIB43A-like with coiled-coils protein 2			72.2	-5.71	n/a	n/a	0.088	0.196	0.031	1.67			
Solute carrier family 13 member 5			80.4	-5.38	-19.83	-106.69	0.009	0.034	0.004	1.68			
Sodium- and chloride-dependent taurine transporter			64.5	1.92	-1.87	1.02	0.338	0.208	0.494	1.69			
Saccharopine dehydrogenase-like oxidoreductase			94.7	-1.34	1.22	-1.09	0.192	0.255	0.193	1.70			
Sortilin precursor			66.7	1.22	-1.25	-1.02	0.268	0.287	0.478	1.71			
Signal peptide peptidase-like 2B			75.0	2.05	-1.72	1.20	0.163	0.285	0.357	1.72			
			54.1	-1.00	1.44	1.44	0.495	0.054	0.044	1.73			
			54.7	2.01	1.38	2.78	0.214	0.248	0.052	1.74			
			91.4	-2.31	2.75	1.19	0.078	0.050	0.291	1.75			
			53.6	ND	ND	ND	ND	ND	ND	1.76			
			42.3	1.39	1.53	2.13	0.242	0.063	0.028	1.77			
			98.5	-1.24	1.30	1.05	0.409	0.321	0.457	1.78			
			57.9	ND	ND	ND	ND	ND	ND	1.79			
			81.5	1.35	2.14	2.89	0.130	0.059	0.023	1.80			
			61.7	1.48	-1.04	1.41	0.070	0.450	0.283	1.81			
			98.0	1.09	1.78	1.94	0.455	0.169	0.273	1.82			

TABLE 1. Continued.

Peptide	Peptide sequence <sup>a</sup>	Lectin binding		Mascot score	Fold change <sup>b</sup>			P value <sup>b</sup>		MS/MS <sup>c</sup>	
		SNA	WGA		Caput vs. corpus	Corpus vs. cauda	Caput vs. cauda	Corpus vs. cauda	Caput vs. cauda		
											Caput vs. corpus
Testis-expressed sequence 29 protein	K:TFAVCDISILYDIDCVNVR.D			89.8	2.10	-1.88	1.11	0.151	0.191	0.392	1.83
Tripeptidyl-peptidase 2	R:KQEEFDIANNGSSQANK.L			80.2	1.20	-1.54	-1.29	0.351	0.275	0.250	1.84
Protein-tyrosine sulfotransferase 2	R:LGYDPYANPNYGNPDPIVNNTHR.V			44.5	ND	ND	ND	ND	ND	ND	1.85
Testis-expressed protein 101 precursor	R:NNLASILQAPEPTATNMSGAR.H			65.6	-1.74	-3.42	-5.95	0.047	0.015	0.014	1.86
	R:TLSLEDNPSGTFNWSK.A			95.0	-2.07	-2.93	-6.07	0.051	0.060	0.016	1.87
	K:AVCPKEIINGNLSVEK.E			62.3	-1.03	-1.13	-1.16	0.443	0.115	0.219	1.88
Zona pellucida sperm-binding protein 3 receptor precursor	K:GVNWSDSLPECVIATCEPPVINGK.H *			37.1	ND	ND	ND	ND	ND	ND	1.89
Zona pellucida-binding protein 2 precursor	R:ANVHDVQIVTCQENLWSSPSCCER.V *			96.5	1.29	-1.15	1.12	0.097	0.090	0.133	1.90
	R:TNSSHITCDENGS <del>W</del> VVYTF <del>C</del> AR.K *			46.5	ND	ND	ND	ND	ND	ND	1.91
	K:SMCNSSMDCEDVTNHNILK.A *			74.8	1.02	-1.05	-1.03	0.482	0.451	0.447	1.92

<sup>a</sup> Consensus sequence for N-glycosylation is shown underlined and in boldface. The period between the first and second residue indicates the trypsin cleavage site.

<sup>b</sup> ND (not determined) is used when the area under the curve could not be measured in all samples; n/a (not applicable) is used when the mean area of one or both regions of the epididymis was equal to zero.

<sup>c</sup> Numbers in MS/MS column correspond to the numbers within Supplemental Fig. S1 that contains MS/MS spectrum of the glycopeptides.

\* Ambiguous localization of deamidated residue.

488 donkey anti-goat IgG (Life Technologies) in a 1:100 dilution with PBS containing 1% (w/v) BSA. After incubation, the coverslips were washed and mounted with Mowiol medium. Cells were evaluated using phase contrast and epifluorescence microscopy. As a control, a blocking peptide specific to anti-Basigin (1:25 dilution) was incubated for 5 min before addition of primary antibodies to the cells.

## RESULTS

### *N-Linked Sialylated Glycoproteins Identified by LC-MS/MS*

The protocol used in the present study is based upon the use of TiO<sub>2</sub> and PNGase F to selectively enrich for *N*-linked sialylated glycopeptides. Following treatment with alkaline phosphatase, samples were incubated with TiO<sub>2</sub> to enrich for negatively charged compounds, including Sia residues. Addition of PNGase F to washed beads then cleaves *N*-linked glycans (between the innermost GlcNAc and Asparagine residue), releasing the peptide backbone and promoting a mass increase of 0.98 Da due to Asparagine deamidation. Following this protocol, we initially identified a total of 270 nonredundant peptides. Despite the fact that PNGase F was used to elute the peptides, the analysis of each peptide sequence revealed that 136 (50.4%) of them had no *N*-linked consensus sequence (NXS/T) and as such were immediately discarded. Manual inspection of the MS/MS data from the tryptic peptides containing a consensus sequence plus a deamidation event revealed three possible outcomes. First, those peptides with unambiguous Asparagine deamidation within the consensus site were taken as potentially glycosylated. Second, peptides with a known deamidation event, which could not be clearly annotated with the MS/MS spectra (ambiguous) due to the lack of an Asparagine *y*- or *b*- ion, were also reported as glycosylated. These peptides are clearly marked (asterisk) in Table 1 because some of them may be false positives. Third, peptides in which the MS/MS data revealed deamidated residues not within the N-glycan consensus sequence were excluded. Table 1 lists the 92 unique glycopeptides from 63 different proteins that met these criteria.

The MS/MS spectrum from all peptides shown in Table 1 can be found in Supplemental Figure S1 (Supplemental Data are available online at [www.biolreprod.org](http://www.biolreprod.org)). Additional MS technical information regarding the sialylated N-glycopeptides identified, including m/z values obtained in MS analysis (measured) or calculated based on the known peptide sequence and peptide charge and retention times, are presented in Supplemental Table S1.

### *Lectin Affinity Chromatography*

Previous studies have shown that lectins can have some affinity for Sia. For example, WGA and SNA have both been shown to have some specificity for Sia [1]. However, it does need to be recognized that these lectins can also bind other sugar groups. For example, WGA also has specificity toward GlcNAc [1]. Nevertheless, to compare the specificity of these lectins and to see if they could enrich for similar proteins as observed for the TiO<sub>2</sub> protocol, rat sperm cell lysates were incubated with both lectins and, after elution, binding proteins were identified by tandem MS. Only ~10% of the proteins found in the TiO<sub>2</sub> study were also found with lectin binding. Several nonspecific (nonglycosylated) proteins were also found to bind lectins, including large families of histones. Those proteins identified by both TiO<sub>2</sub> and either SNA or WGA are labeled in Table 1. Given that we had both a glycan consensus site (NXS/T) and elution from TiO<sub>2</sub> using PNGase F, we decided to continue further looking at the TiO<sub>2</sub>-enriched peptides.

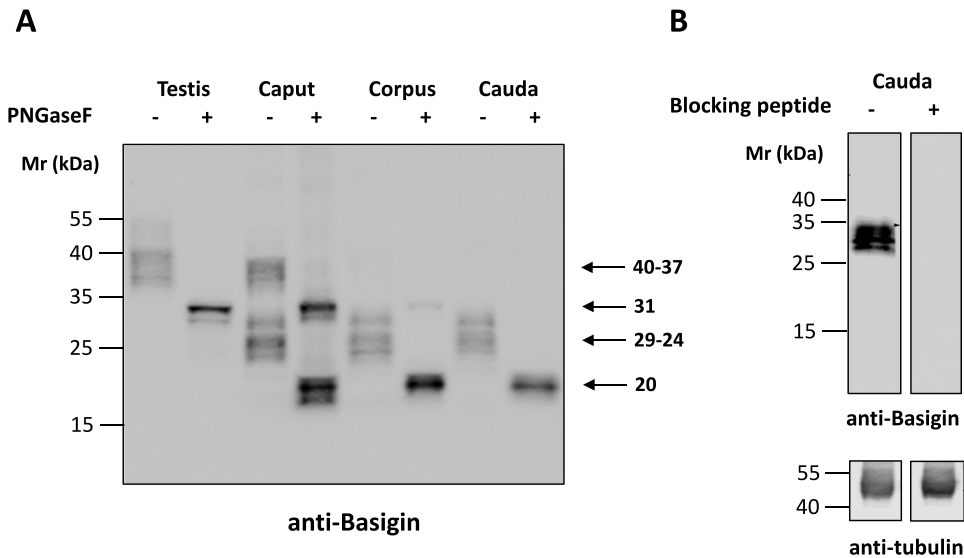


FIG. 2. Western blot analysis of rat testicular (testis) and epididymal sperm (caput, corpus, and cauda) proteins extracted with CHAPS lysis buffer. **A)** Proteins (10  $\mu$ g/lane) treated (+) or nontreated (-) with PNGase F (385 U/ml, overnight) were probed with anti-Basigin. **B)** Anti-Basigin antibody was incubated with the vehicle control (left-hand side) or blocking peptide (right-hand side) for 5 min before being added to the membrane. To demonstrate equal amounts of protein, the membranes were stripped and re probed for anti-antibody.

#### Label-Free Quantification and Gene Ontology of the N-Linked Sialylated Glycoproteins

Using MS-based label-free quantification as previously described for the sperm phosphoproteome [38, 39], the  $\text{TiO}_2$ -enriched sialylated N-glycopeptides identified by MS/MS in rat epididymal spermatozoa were compared among the different regions of the epididymis (caput vs. corpus vs. cauda). As a result, 52.2% (48/92) of the peptides, identified on 37 sialoglycoproteins, underwent changes in their amount as the sperm cells transited through the epididymis (Table 1). The sialoglycoproteins regulated during epididymal maturation were then categorized according to their molecular function and biological process properties using Gene Ontology (<http://www.geneontology.org>; see [40]). Results are shown as a pie chart in Figure 1. Only proteins with available annotation were considered. Regarding molecular function, a high percentage of the sialylated glycoproteins had catalytic (40%), binding (23.3%), or receptor (16.7%) activities. Nevertheless, these proteins showed some diversity in their biological function with metabolic process (19.8%), cellular process (12.3%), developmental process (11.1%), and reproduction (9.9%) accounting for a little over half.

#### Enzymatic Deglycosylation of the N-Linked Sialoglycoproteins Identified

To substantiate the findings from the LC-MS/MS analysis, three of the glycoproteins identified in the current study were chosen for further study using PNGase F deglycosylation. One protein for each of the following cases was selected: protein known to be 1) processed within sperm cells (Basigin, also called CE9 in the rat) [40], 2) incorporated into spermatozoa (ADAM7, also called EAP I) [41], or 3) released from spermatozoa (TEX101; information based on mouse sperm study) [42] during epididymal transit.

#### Decrease in Basigin Mass Following PNGase F Treatment

The predicted polypeptide sequence of Basigin in rats reveals the presence of three potential N-glycosylation sites within the Ig-like domains (N160 at the C2-like Ig domain and N269 and N305 at the V-type Ig domain). Of interest, all three potential glycosylation sites were identified by our MS/MS analysis, suggesting the presence of Sia-containing glycans in all sites (Table 1). The tryptic peptide containing the glycosylation site N160, belonging to the C2-like Ig domain, was found only in caput samples whereas the N269 site, from the V-type Ig domain, was equally present in all epididymal regions (Table 1). Immunoblotting analysis of Basigin indicates that this protein undergoes proteolytic cleavage within the caput region (Fig. 2A). Taken together, immunoblotting and MS analyses strongly suggest that the Ig-like C2-type domain is lost at the initial segments of the epididymis. This proteolytic processing of Basigin is known to coincide with a progressive shift in the location of this protein from the posterior to the anterior tail region of rat sperm [40]. Our data confirm this. The final location of Basigin is shown in Figure 3. Despite the epididymal processing of Basigin, deglycosylation with PNGase F demonstrated that N-glycans are always present in Basigin, regardless of the epididymal region (Fig. 2A). This fact corroborates with our finding that the glycosylation site N269 was constant among the different regions of the epididymis.

#### Decrease in ADAM7 Mass Following PNGase F Treatment

To achieve successful deglycosylation of ADAM7, proteins extracted in 2% (w/v) SDS buffer were submitted to an overnight incubation with high concentrations of PNGase F (770 U/ml). Because ADAM7 is produced in the epididymides, we also subjected epididymal tissue homogenates to PNGase F treatment before probing with anti-ADAM7 antibody. Using antibodies raised against ADAM7, we found three cross-reacting bands present at 110, 85, and 42 kDa within rat caudal epididymal spermatozoa (Fig. 4A, lanes 1 and 2). As a comparison, ADAM7 from epididymal epithelial cells is shown

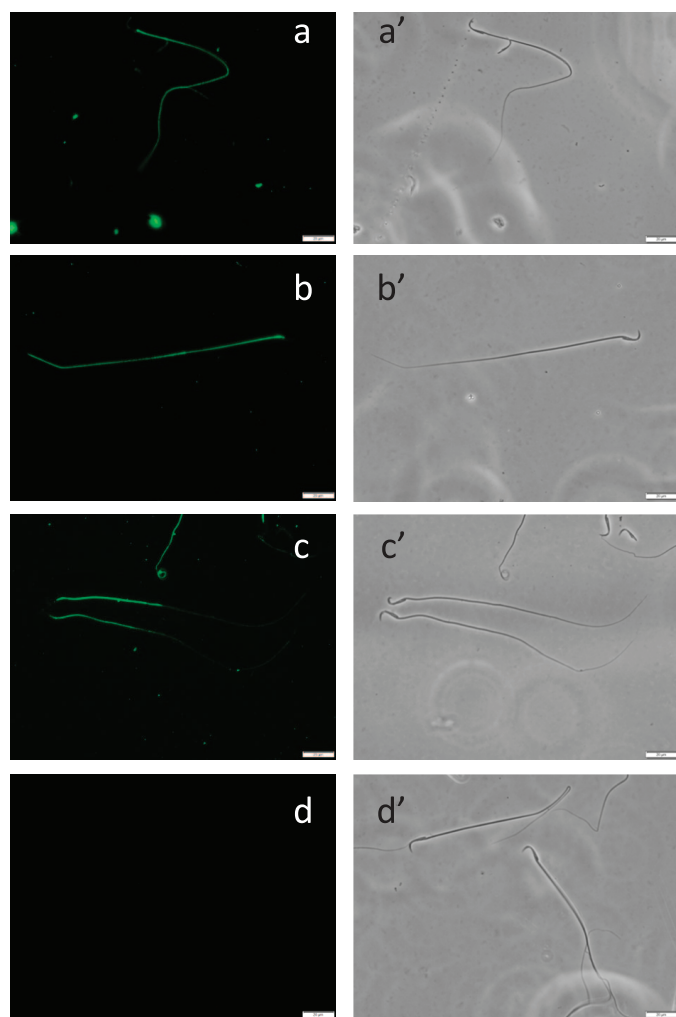


FIG. 3. Immunofluorescent localization of Basigin and the corresponding phase-contrast micrographs of rat spermatozoa retrieved from three regions of the epididymis; caput (a, a'), corpus (b, b'), and cauda (c, c'). Spermatozoa were fixed in 4% formaldehyde, immobilized on precoated slides, permeabilized with 0.2% saponin, and incubated overnight with anti-Basigin antibody. Alexa Fluor 488-conjugated secondary antibody (green) was used for detection of the primary antibody. Primary antibody was incubated with blocking peptide in control (d, immunofluorescence; d', phase-contrast). Bar = 50.0  $\mu$ m.

(Fig. 4A, lanes 3 and 4). Due to low amounts of ADAM7 in sperm cells, prolonged exposure of the immunoblot was necessary in order to visualize this protein (Fig. 4A). Nevertheless, it was possible to note that enzymatic deglycosylation of ADAM7 from both cauda sperm and epididymal tissue resulted in the reduction of its molecular weight (MW) (from 110 kDa to 97 kDa), confirming the presence of *N*-linked glycans. To demonstrate the specificity of the antibody, anti-ADAM7 was preincubated with either the vehicle or the blocking peptide before probing caudal-derived sperm cell lysates (Fig. 4B). As shown, no signal was obtained in the presence of the blocking peptide, suggesting that the antibody was specific to ADAM7.

#### No Change in Mass of Rat Epididymal TEX101 Following PNGase F Treatment

Although the majority of the TEX101 protein in mouse sperm is known to be released during epididymal transit [42],

we observed that rat samples from cauda sperm still show high amounts of this protein (Fig. 5A), demonstrating a difference between mouse and rat sperm maturation. Interestingly, despite the fact that tryptic peptides from TEX101 were successfully deglycosylated by PNGase F (Table 1), this enzyme was unable to promote deglycosylation of the nondigested TEX101 extracted from epididymal sperm (Fig. 5A). In contrast, when TEX101 from rat testis homogenates was submitted to deglycosylation with PNGase F, a shift in mass from  $\sim$ 48 to  $\sim$ 42 kDa was observed (Fig. 5A). Notably, this was the same MW found for TEX101 in all epididymal sperm samples, regardless of PNGase F treatment. Considering that the predicted size of the polypeptide backbone of TEX101 is around 24 kDa (nonglycosylated), an incomplete enzymatic digestion of testis samples is a likely explanation. Surprisingly, this resistance to PNGase F seems to be species dependent. When the same deglycosylation conditions were applied to mouse testicular tissue homogenates, we obtained a reduction of TEX101 mass to values close to its predicted amino acid sequence size (24 kDa; Fig. 5B).

To investigate whether the resistance to PNGase F was an artifact of the protocol, we tested alterations in the deglycosylation protocol such as the use of different detergents (Triton X-100 or NP-40) and denaturing conditions (DTT or 2-mercaptoethanol) as well as high enzyme concentrations (385–770 U/ml) and long incubation periods (up to 68 h). However, no change in the mass of TEX101 from rat epididymal sperm was observed under any of the conditions tested here (data not shown). Preincubation of TEX-101 with either the vehicle (Fig. 5C) or the blocking peptide before probing caudal-derived sperm cell lysates demonstrated the antibody's specificity.

#### Immunolocalization of TEX101 in Rat Sperm

Considering that TEX101 from testicular homogenates showed higher MW compared to epididymal spermatozoa, immunofluorescence studies were performed to investigate whether this was related to changes in protein localization. Regardless of the cell type, immunoreactivity for TEX101 was observed in all sperm tail, with the midpiece region showing stronger staining (Fig. 6, a–d). The highest immunoreactivity to TEX101 was noted in the cytoplasmic droplet (Fig. 6, a and c). Although the sperm head from all samples were positively stained for TEX101 (Fig. 6, a–d), testicular sperm showed a more uniform immunoreactive distribution over the entire head (Fig. 6a), whereas some variations in the staining pattern were observed for the epididymal spermatozoa. As spermatozoa passed from the caput to the cauda epididymis, TEX101 staining showed a tendency to concentrate in the ventral portion of the sperm heads. As a result, a strong immunoreactive line could be seen in the caput (12%) and especially in the corpus (71%) and cauda (82%) cells (Fig. 6, b–d). Nevertheless, immunostaining of the postacrosomal region was still observed in some cells (Fig. 6d). Controls incubated with blocking peptide showed no signal (Fig. 6, i–l).

#### DISCUSSION

In order to acquire fertilizing capacity, spermatozoa undergo modifications during epididymal transit that include changes in protein glycosylation [18–21, 43]. With this in mind, LC-MS/MS analysis in combination with TiO<sub>2</sub> enrichment was successfully used in the present study to investigate the sialylated *N*-glycoproteome dynamics of rat spermatozoa during epididymal maturation. This approach allowed the identification of 92 unique formerly *N*-linked glycopeptides

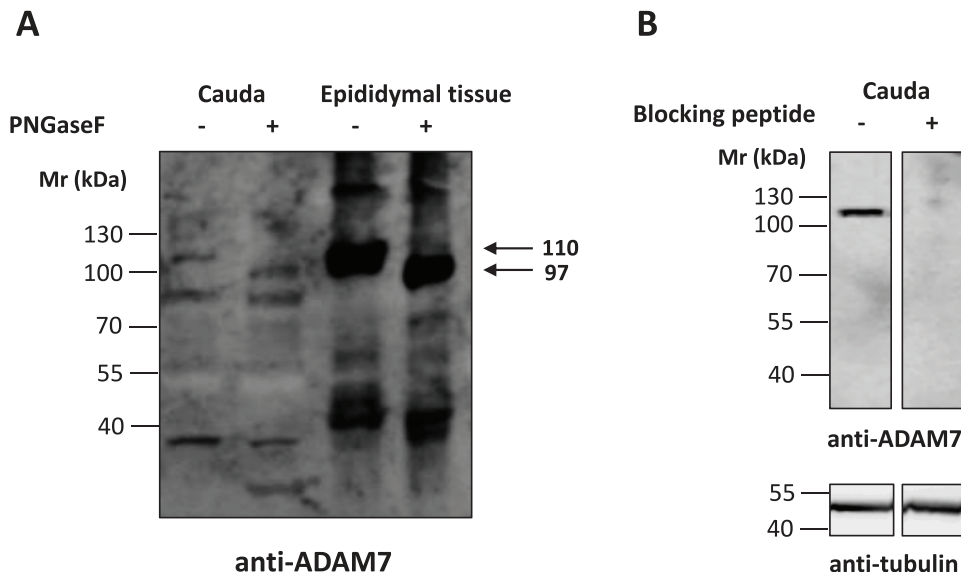


FIG. 4. **A**) Western blot analysis of proteins from cauda sperm (40 µg/lane) and epididymal tissue (12 µg/lane) extracted with SDS Tris buffer and treated (+) or nontreated (-) with PNGase F (770 U/ml, overnight). Membrane was probed with anti-ADAM7 antibody. **B**) Anti-ADAM7 antibody was incubated with the vehicle control (left-hand side) or blocking peptide (right-hand side) for 5 min before being added to the membrane. To demonstrate equal amounts of protein, the membranes were stripped and reprobbed for anti- $\alpha$ -tubulin.

potentially containing terminal Sia, with around half of them being regulated during maturation.

Although the protocol used in this study enriched for N-glycopeptides, only 34.1% (92/270) of the peptides identified by MS/MS could be annotated as potential sialylated N-glycopeptides. Enrichment using TiO<sub>2</sub> is based on the presence of negative charges on the peptide structure. Therefore, to avoid copurification of peptides containing phosphate groups and acidic amino acids, peptides were treated with alkaline phosphatase and then submitted to highly acid conditions during the binding step. Although the later should render Aspartic and Glutamic acids free of charge, peptides containing these residues and no indication of N-linked sugars (no

consensus sequence and a deamidation event) were observed. Elution of these peptides may be a consequence of the pH adjustment (pH ~7.0) necessary for optimal PNGase F treatment. Indeed, others have shown several different conformations of Glutamic acid in particular absorb on the TiO<sub>2</sub> surface as the pH is adjusted from acidic to neutral [44]. The presence of contaminants (23.3%) has also been reported by Palmisano et al. [35] when using similar enrichment protocol. Moreover, the proportion of contaminants seems to be related to the cell type. Of particular interest, in trials performed with liver samples, we observed lower percentage of nonglycosylated peptides when compared to the sperm samples (data not shown).

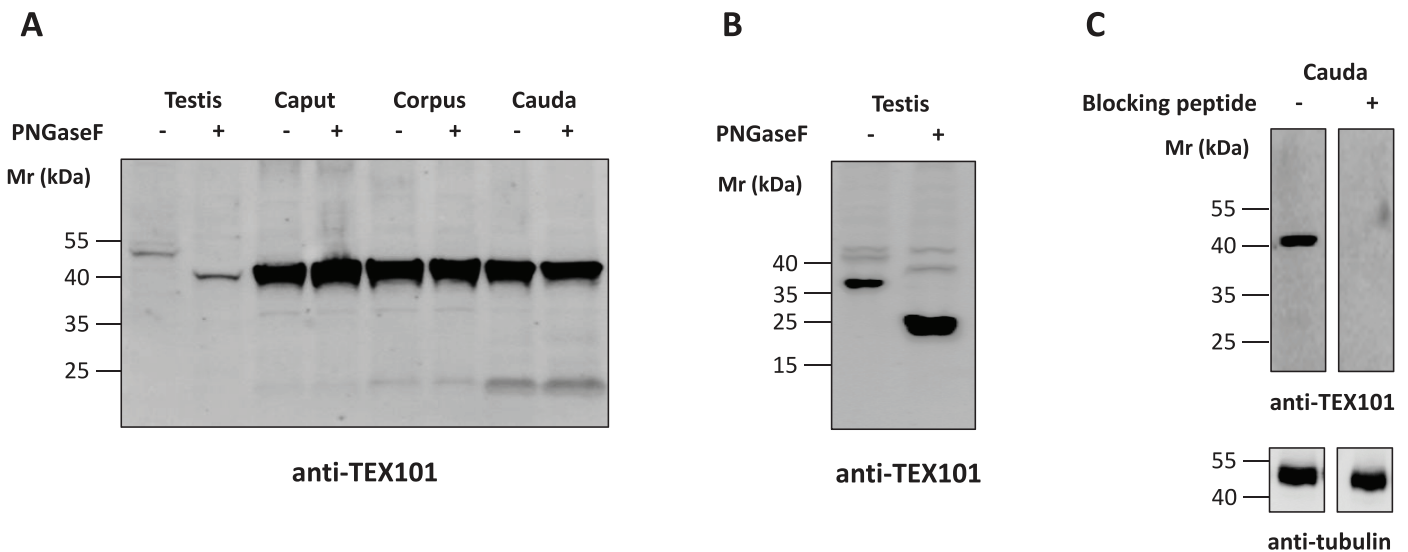


FIG. 5. Rat testicular tissue and epididymal sperm (caput, corpus, and cauda; **A**) and mouse testicular tissue (**B**) were submitted to immunoblot analysis. Proteins were extracted using CHAPS lysis buffer and then treated (+) or nontreated (-) overnight with PNGase F (160 U/ml for mouse samples and 385 U/ml for rat samples). Proteins (10 µg/lane) were separated by SDS-PAGE and probed with the anti-TEX101 antibody. **C**) Anti-TEX101 antibody was incubated with the vehicle control (left-hand side) or blocking peptide (right-hand side) for 5 min before being added to the membrane. To demonstrate equal amounts of protein, the membranes were stripped and reprobbed for anti- $\alpha$ -tubulin.

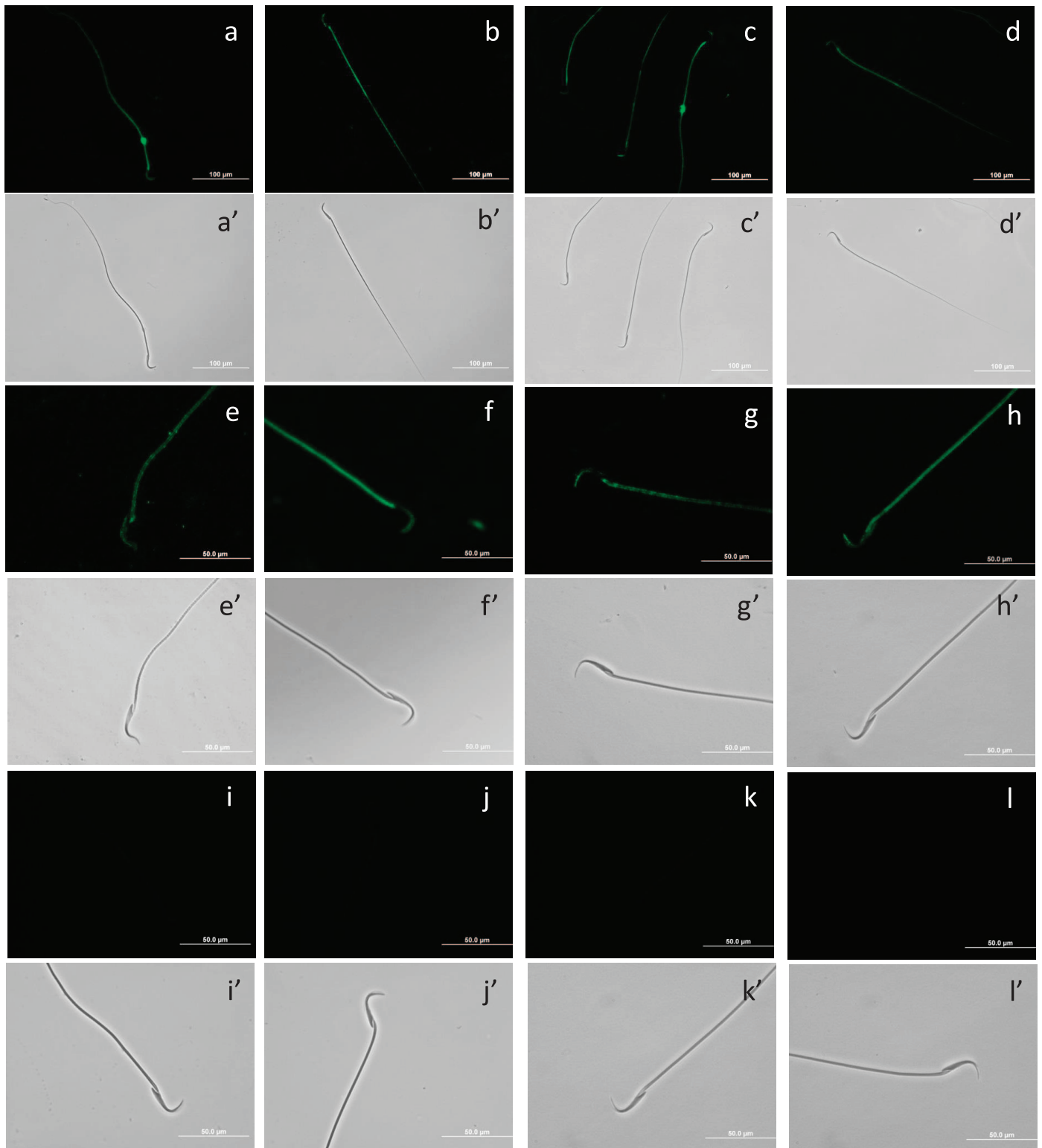


FIG. 6. Immunofluorescent localization of TEX101 and the corresponding phase-contrast micrographs of rat spermatozoa retrieved from testis (**a**, **a'**, **e**, **e'**) and three regions of the epididymis; caput (**b**, **b'**, **f**, **f'**), corpus (**c**, **c'**, **g**, **g'**), and cauda (**d**, **d'**, **h**, **h'**). Spermatozoa were fixed in 4% formaldehyde, immobilized on precoated slides, permeabilized with 0.2% saponin, and incubated overnight with anti-TEX101 antibody. Alexa Fluor 488-conjugated secondary antibody (green) was used for detection of the primary antibody. Primary antibody was omitted in control (**i-l**, immunofluorescence; **i'-l'**, phase-contrast).

Several of these glycoproteins are known to be involved in sperm migration into the female tract as well as in sperm-egg interaction. For instance, five members of the disintegrin and metalloprotease domain-containing protein (ADAM) family

(ADAM1, ADAM2, ADAM5, ADAM7, and ADAM18) were found. These proteins contained one to three N-glycosylation sites, and at least one glycopeptide from each one of them was shown to be regulated during epididymal transit (Table 1).

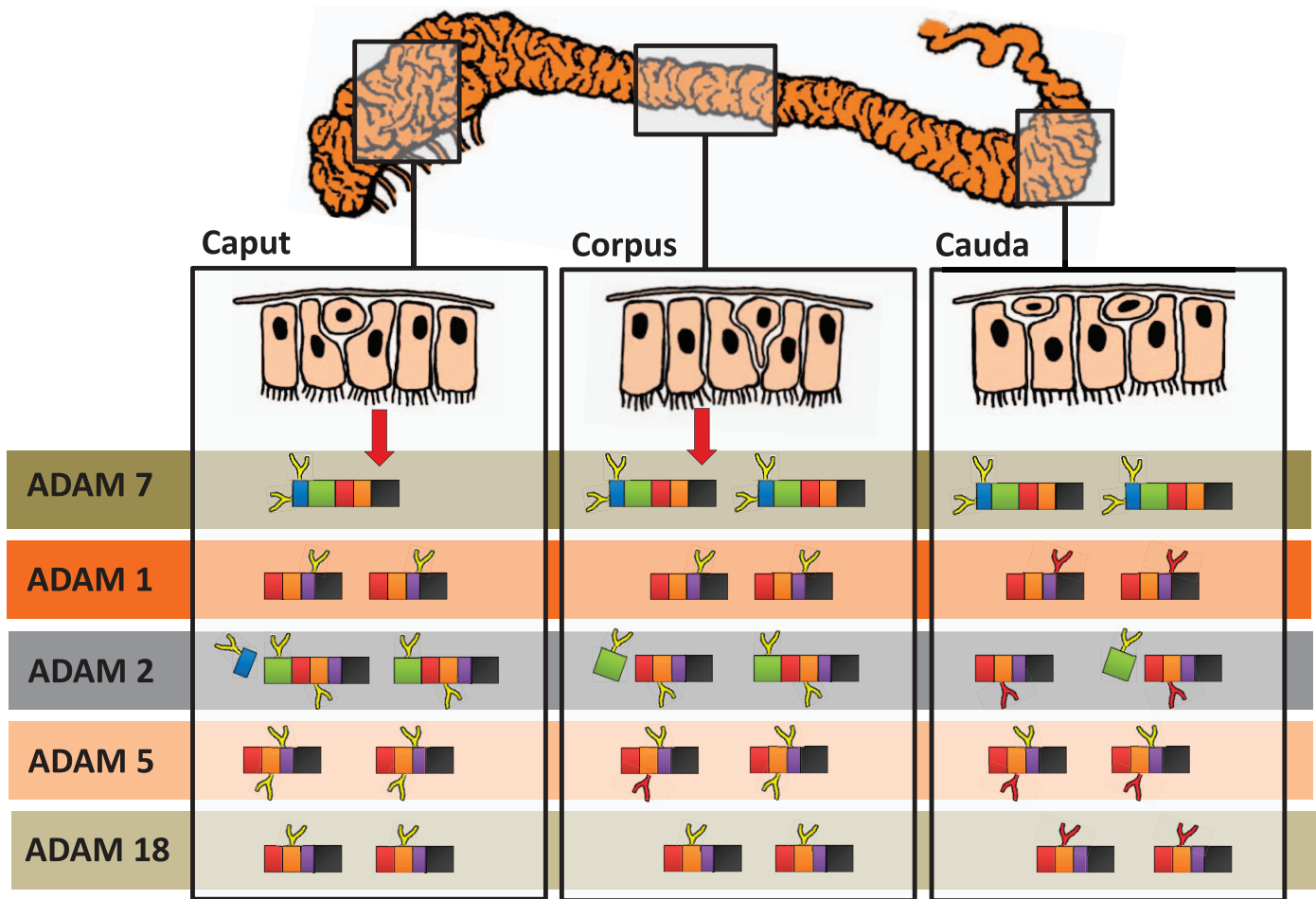


FIG. 7. A model depicting ADAM family processing during epididymal maturation. The model demonstrates changes that occur within ADAM isoforms and is based on the current and literature studies for both rat and mice.

Combining the information obtained herein with those already published for rats and mice, we established a model (Fig. 7) for the processing of some ADAM members during the epididymal maturation of rat sperm. In the case of ADAM7, previous studies have demonstrated that this protein is synthesized in the epididymis [41, 45, 46] and then transferred to spermatozoa by epididymosomes [47]. Indeed, in the present study, two N-glycosylation sites (N84 and N167), belonging to the prodomain region, increased as sperm passed through the epididymis. In addition, using enzymatic deglycosylation, we confirmed the presence of glycan structures within rat ADAM7. These results are consistent with the fact that ADAM7 can be labeled with WGA [20] and is not proteolytically cleaved during sperm maturation [41, 48].

Unlike ADAM7, other members of the family are processed in the epididymis, losing their pro- and metalloprotease domains. According to our data, ADAM2 contains one N-glycan moiety in each of these domains (Table 1 and Fig. 7). The peptides containing these glycan structures decreased in a temporal fashion, first, the one embedded in the prodomain (N128) and then the one within the metalloprotease domain (N359) during maturation (see Fig. 7), which likely corresponds to a step-by-step processing of ADAM2 as described in other species [49, 50].

In the current study, three members of the ADAM family (ADAM2, ADAM5, and ADAM18) exhibited one Sia-containing N-glycan (N491, N515, and N340, respectively)

located at the Cysteine-rich domain. Notably, the level of the glycopeptides containing these glycan moieties decreased during sperm maturation (Table 1 and Fig. 7). This reduction could be due to oligosaccharide processing as well as shedding of the proteins ADAM2 and/or ADAM18. In the case of ADAM5, because another glycopeptide had no change during maturation, a modification in the glycan moiety (N515) is the more likely explanation. Despite the importance of the ADAM family members, there is no information regarding the function of their Cysteine-rich domain, which we now have shown to be glycosylated and regulated during epididymal transit. Studies using other ADAM members have indicated a potential role in complementing and/or regulating the binding ability of the disintegrin domain [51–53]. Furthermore, alone or together with the disintegrin domain, the Cysteine-rich domain has shown to act as a ligand for the cell-adhesion molecules Syndecans [54–56], to promote cell adhesion via  $\beta 1$  integrin and to interact with extracellular matrix proteins such as fibronectin [52]. Although not clear from our results, modifications on the glycosylation of the Cysteine-rich domain within these ADAMs may be essential to render sperm cells capable of reaching and fertilizing the oocyte, which would make them potential contraceptive targets.

Previous reports have indicated that TEX101 from mouse and bovine sperm are heavily N-glycosylated [57, 58]. In our study, two N-linked sites containing sialylated N-glycans (N45 and N134) were observed within TEX101 from rat epididymal

sperm. Yet, despite these observations, pretreatment of TEX101 with PNGase F showed no reduction in its MW under several conditions tested. Notably, we achieved complete deglycosylation of TEX101 from mouse testis homogenates and other rat sperm proteins (e.g., Basigin and ADAM7) and partial deglycosylation of TEX101 from rat testicular samples using the same experimental conditions.

Although PNGase F is highly efficient at cleaving all N-glycan types, the presence of an  $\alpha$ -1,3-fucose at the innermost GlcNAc attached to the Asparagine residue is known to abrogate the action of this enzyme [59, 60]. Nevertheless, core  $\alpha$ -1,3-fucose structures have only been reported in plants and some invertebrates [61, 62], suggesting this would be an unlikely mechanism. Interestingly, there is evidence to suggest that some glycoproteins containing carboxylated N-glycans from bovine lung are also PNGase F resistant [63]. As such, resistance to PNGase F could play an essential role at protecting important sperm glycoproteins from the action of glycosidases during epididymal maturation [13, 64]. Indeed, in the case of TEX101, a gene deletion study has proven the importance of this protein for the production of fertile mouse sperm [65].

The results from this work confirm the existence of a maturation-related remodeling of the N-linked sialome in rat spermatozoa and emphasize the importance of MS-based approaches in the study of sperm biology. Among the proteins identified here, several are known to be involved in the fertilizing ability of spermatozoa such as members of the ADAM family. Studies using point mutation of the regulated N-glycans would help to understand the role of these oligosaccharides in sperm function. In addition, the existence of strategies to protect specific oligosaccharide moieties in sperm cells, as observed for bovine lung, needs further investigation. Importantly, the study of such structures may reveal essential epitopes in spermatozoa that could be used in the development of contraceptive methods.

## REFERENCES

- Varki A. Biological roles of oligosaccharides: all of the theories are correct. *Glycobiology* 1993; 3:97–130.
- Ohtsubo K, Marth JD. Glycosylation in cellular mechanisms of health and disease. *Cell* 2006; 126:855–867.
- Tiralongo J, Martinez-Duncker I. *Sialobiology: Structure, Biosynthesis and Function: Sialic Acid Glycoconjugates in Health and Disease*. Oak Park, IL: Bentham Science Publishers; 2013.
- Vancaillie T, Gordts S, Boeckx W, Vasquez G, Brosens I. Vaso-epididymostomy to the head of the epididymis: a comparative study of two microsurgical techniques in the rabbit. *Acta Eur Fertil* 1984; 15:25–29.
- Temple-Smith PD, Zheng SS, Kadioglu T, Southwick GJ. Development and use of surgical procedures to bypass selected regions of the mammalian epididymis: effects on sperm maturation. *J Reprod Fertil Suppl* 1998; 53:183–195.
- Gatti JL, Druart X, Syntin P, Guérin Y, Dacheux JL, Dacheux F. Biochemical characterization of two ram cauda epididymal maturation-dependent sperm glycoproteins. *Biol Reprod* 2000; 62:950–958.
- Saxena DK, Oh-Oka T, Kadomatsu K, Muramatsu T, Toshimori K. Behaviour of a sperm surface transmembrane glycoprotein basigin during epididymal maturation and its role in fertilization in mice. *Reproduction* 2002; 123:435–444.
- Thimon V, Métayer S, Belghazi M, Dacheux F, Dacheux JL, Gatti JL. Shedding of the germinal angiotensin I-converting enzyme (gACE) involves a serine protease and is activated by epididymal fluid. *Biol Reprod* 2005; 73:881–890.
- Tollner TL, Yudin AI, Treece CA, Overstreet JW, Cherr GN. Macaque sperm coating protein DEFB126 facilitates sperm penetration of cervical mucus. *Hum Reprod* 2008; 23:2523–2534.
- Tulsiani DR, Skudlarek MD, Araki Y, Orgebin-Crist MC. Purification and characterization of two forms of beta-D-galactosidase from rat epididymal luminal fluid: evidence for their role in the modification of sperm plasma membrane glycoprotein(s). *Biochem J* 1995; 305:41–50.
- Deng X, Czymbek K, Martin-DeLeon PA. Biochemical maturation of Spam1 (PH-20) during epididymal transit of mouse sperm involves modifications of N-linked oligosaccharides. *Mol Reprod Dev* 1999; 52:196–206.
- Tulsiani DR, Skudlarek MD, Holland MK, Orgebin-Crist MC. Glycosylation of rat sperm plasma membrane during epididymal maturation. *Biol Reprod* 1993; 48:417–428.
- Tulsiani DR. Glycan-modifying enzymes in luminal fluid of the mammalian epididymis: an overview of their potential role in sperm maturation. *Mol Cell Endocrinol* 2006; 250:58–65.
- Bedford JM. Changes in the electrophoretic properties of rabbit spermatozoa during passage through the epididymis. *Nature* 1963; 200:1178–1180.
- Holt WV. Surface-bound sialic acid on ram and bull spermatozoa: deposition during epididymal transit and stability during washing. *Biol Reprod* 1980; 23:847–857.
- Gould KG, Young LG, Hinton BT. Alteration in surface charge of chimpanzee sperm during epididymal transit and at ejaculation. *Arch Androl* 1984; 12(Suppl):9–17.
- Stoffel MH, Busato A, Friess AE. Density and distribution of anionic sites on boar ejaculated and epididymal spermatozoa. *Histochem Cell Biol* 2002; 117:441–445.
- Magargee SF, Kunze E, Hammerstedt RH. Changes in lectin-binding features of ram sperm surfaces associated with epididymal maturation and ejaculation. *Biol Reprod* 1988; 38:667–685.
- Kumar GP, Laloraya M, Agrawal P, Laloraya MM. The involvement of surface sugars of mammalian spermatozoa in epididymal maturation and in vitro sperm-zona recognition. *Andrologia* 1990; 22:184–194.
- Liu HW, Wang JJ, Chao CF, Muller C. Identification of two maturation-related, wheat-germ-lectin-binding proteins on the surface of mouse sperm. *Acta Anat (Basel)* 1991; 142:165–170.
- Navaneetham D, Sivashanmugam P, Rajalakshmi M. Changes in binding of lectins to epididymal, ejaculated, and capacitated spermatozoa of the rhesus monkey. *Anat Rec* 1996; 245:500–508.
- Lassalle B, Testart J. Human zona pellucida recognition associated with removal of sialic acid from human sperm surface. *J Reprod Fertil* 1994; 101:703–711.
- Bernal A, Torres J, Reyes A, Rosado A. Presence and regional distribution of sialyl transferase in the epididymis of the rat. *Biol Reprod* 1980; 23:290–293.
- Steele MG, Wishart GJ. Demonstration that the removal of sialic acid from the surface of chicken spermatozoa impedes their transvaginal migration. *Theriogenology* 1996; 46:1037–1044.
- Toshimori K, Araki S, Oura C, Eddy EM. Loss of sperm surface sialic acid induces phagocytosis: an assay with a monoclonal antibody T21, which recognizes a 54K sialoglycoprotein. *Arch Androl* 1991; 27:79–86.
- Yudin AI, Generao SE, Tollner TL, Treece CA, Overstreet JW, Cherr GN. Beta-defensin 126 on the cell surface protects sperm from immunorecognition and binding of anti-sperm antibodies. *Biol Reprod* 2005; 73:1243–1252.
- Tollner TL, Yudin AI, Tarantal AF, Treece CA, Overstreet JW, Cherr GN. Beta-defensin 126 on the surface of macaque sperm mediates attachment of sperm to oviductal epithelia. *Biol Reprod* 2008; 78:400–412.
- Ma F, Wu D, Deng L, Secrest P, Zhao J, Varki N, Lindheim S, Gagneux P. Sialidases on mammalian sperm mediate deciduous sialylation during capacitation. *J Biol Chem* 2012; 287:38073–38079.
- Alvarez-Manilla G, Atwood J III, Guo Y, Warren NL, Orlando R, Pierce M. Tools for glycoproteomic analysis: size exclusion chromatography facilitates identification of tryptic glycopeptides with N-linked glycosylation sites. *J Proteome Res* 2006; 5:701–708.
- Baker MA, Krutskikh A, Curry BJ, McLaughlin EA, Aitken RJ. Identification of cytochrome P450-reductase as the enzyme responsible for NADPH-dependent lucigenin and tetrazolium salt reduction in rat epididymal sperm preparations. *Biol Reprod* 2004; 71:307–318.
- Baker MA, Krutskikh A, Curry BJ, Hetherington L, Aitken RJ. Identification of cytochrome-b5 reductase as the enzyme responsible for NADH-dependent lucigenin chemiluminescence in human spermatozoa. *Biol Reprod* 2005; 73:334–342.
- Biggers JD, Whitten WK, Whittingham DG. The culture of mouse embryos in vitro. In: Daniel JC (ed.), *Methods in Mammalian Embryology*. San Francisco, CA: WH Freeman; 1971:86–116.
- Baker MA, Witherdin R, Hetherington L, Cunningham-Smith K, Aitken RJ. Identification of post-translational modifications that occur during sperm maturation using difference in two-dimensional gel electrophoresis. *Proteomics* 2005; 5:1003–1012.
- Wessel D, Fugge UI. A method for the quantitative recovery of protein in

- dilute solution in the presence of detergents and lipids. *Anal Biochem* 1984; 138:141–143.
35. Palmisano G, Lendal SE, Engholm-Keller K, Leth-Larsen R, Parker BL, Larsen MR. Selective enrichment of sialic acid-containing glycopeptides using titanium dioxide chromatography with analysis by HILIC and mass spectrometry. *Nat Protoc* 2010; 5:1974–1982.
  36. Baker MA, Naumovski N, Hetherington L, Weinberg A, Velkov T, Aitken RJ. Head and flagella subcompartmental proteomic analysis of human spermatozoa. *Proteomics* 2013; 13:61–74.
  37. Gallagher JT, Morris A, Dexter TM. Identification of two binding sites for wheat-germ agglutinin on polylectosamine-type oligosaccharides. *Biochem J* 1985; 231:115–122.
  38. Baker MA, Smith ND, Hetherington L, Pelzing M, Condina MR, Aitken RJ. Use of titanium dioxide to find phosphopeptide and total protein changes during epididymal sperm maturation. *J Proteome Res* 2011; 10:1004–1017.
  39. Baker MA, Smith ND, Hetherington L, Taubman K, Graham ME, Robinson PJ, Aitken RJ. Label-free quantitation of phosphopeptide changes during rat sperm capacitation. *J Proteome Res* 2010; 9:718–729.
  40. Petruszak JA, Nehme CL, Bartles JR. Endoproteolytic cleavage in the extracellular domain of the integral plasma membrane protein CE9 precedes its redistribution from the posterior to the anterior tail of the rat spermatozoon during epididymal maturation. *J Cell Biol* 1991; 114:917–927.
  41. Pery AC, Jones R, Barker PJ, Hall L. A mammalian epididymal protein with remarkable sequence similarity to snake venom haemorrhagic peptides. *Biochem J* 1992; 286:671–675.
  42. Takayama T, Mishima T, Mori M, Ishikawa T, Takizawa T, Goto T, Suzuki M, Araki Y, Matsubara S, Takizawa T. TEX101 is shed from the surface of sperm located in the caput epididymidis of the mouse. *Zygote* 2005; 13:325–333.
  43. Fàbrega A, Puigmulé M, Dacheux JL, Bonet S, Pinart E. Glycocalyx characterisation and glycoprotein expression of *Sus domesticus* epididymal sperm surface samples. *Reprod Fertil Dev* 2012; 24:619–630.
  44. Roddick-Lanzilotta AD, McQuillan AJ. An in situ infrared spectroscopic study of glutamic acid and of aspartic acid adsorbed on TiO<sub>2</sub>: implications for the biocompatibility of titanium. *J Colloid Interface Sci* 2000; 227:48–54.
  45. Cornwall GA, Hsia N. ADAM7, a member of the ADAM (a disintegrin and metalloprotease) gene family is specifically expressed in the mouse anterior pituitary and epididymis. *Endocrinology* 1997; 138:4262–4272.
  46. Liu HW, Lin YC, Chao CF, Chang SY, Sun GH. GP-83 and GP-39, two glycoproteins secreted by human epididymis are conjugated to spermatozoa during maturation. *Mol Hum Reprod* 2000; 6:422–428.
  47. Oh JS, Han C, Cho C. ADAM7 is associated with epididymosomes and integrated into sperm plasma membrane. *Mol Cells* 2009; 28:441–446.
  48. Oh J, Woo JM, Choi E, Kim T, Cho BN, Park ZY, Kim YC, Kim DH, Cho C. Molecular, biochemical, and cellular characterization of epididymal ADAMs, ADAM7 and ADAM28. *Biochem Biophys Res Commun* 2005; 331:1374–1383.
  49. Kim T, Oh J, Woo JM, Choi E, Im SH, Yoo YJ, Kim DH, Nishimura H, Cho C. Expression and relationship of male reproductive ADAMs in mouse. *Biol Reprod* 2006; 74:744–750.
  50. Fàbrega A, Guyonnet B, Dacheux JL, Gatti JL, Puigmulé M, Bonet S, Pinart E. Expression, immunolocalization and processing of fertilins ADAM-1 and ADAM-2 in the boar (*Sus domesticus*) spermatozoa during epididymal maturation. *Reprod Biol Endocrinol* 2011; 9:96.
  51. Zolkiewska A. Disintegrin-like/cysteine-rich region of ADAM 12 is an active cell adhesion domain. *Exp Cell Res* 1999; 252:423–431.
  52. Gaultier A, Cousin H, Darribere T, Alfandari D. ADAM13 disintegrin and cysteine-rich domains bind to the second heparin-binding domain of fibronectin. *J Biol Chem* 2002; 277:23336–23344.
  53. Smith KM, Gaultier A, Cousin H, Alfandari D, White JM, DeSimone DW. The cysteine-rich domain regulates ADAM protease function in vivo. *J Cell Biol* 2002; 159:893–902.
  54. Iba K, Albrechtsen R, Gilpin BJ, Loechel F, Wewer UM. Cysteine-rich domain of human ADAM 12 (meltrin alpha) supports tumor cell adhesion. *Am J Pathol* 1999; 154:1489–1501.
  55. Iba K, Albrechtsen R, Gilpin B, Fröhlich C, Loechel F, Zolkiewska A, Ishiguro K, Kojima T, Liu W, Langford JK, Sanderson RD, Brakebusch C, et al. The cysteine-rich domain of human ADAM 12 supports cell adhesion through syndecans and triggers signaling events that lead to beta1 integrin-dependent cell spreading. *J Cell Biol* 2000; 149:1143–1156.
  56. Thodeti CK, Albrechtsen R, Grauslund M, Asmar M, Larsson C, Takada Y, Mercurio AM, Couchman JR, Wewer UM. ADAM12/syndecan-4 signaling promotes beta 1 integrin-dependent cell spreading through protein kinase Calpha and RhoA. *J Biol Chem* 2003; 278:9576–9584.
  57. Jin H, Yoshitake H, Tsukamoto H, Takahashi M, Mori M, Takizawa T, Takamori K, Ogawa H, Kinoshita K, Araki Y. Molecular characterization of a germ-cell-specific antigen, TEX101, from mouse testis. *Zygote* 2006; 14:201–208.
  58. Nagdas SK, McLean EL, Richardson LP, Raychoudhury S. Identification and characterization of TEX101 in bovine epididymal spermatozoa. *Biochem Res Int* 2014; 2014:573293.
  59. Tretter V, Altmann F, März L. Peptide-N4-(N-acetyl-beta-glucosaminy-l)asparagine amidase F cannot release glycans with fucose attached alpha 1-3 to the asparagine-linked N-acetylglucosamine residue. *Eur J Biochem* 1991; 199:647–652.
  60. Altmann F, Schweitzer S, Weber C. Kinetic comparison of peptide: N-glycosidases F and A reveals several differences in substrate specificity. *Glycoconj J* 1995; 12:84–93.
  61. Fabini G, Freilinger A, Altmann F, Wilson IB. Identification of core alpha 1,3-fucosylated glycans and cloning of the requisite fucosyltransferase cDNA from *Drosophila melanogaster*. Potential basis of the neural anti-horseradish peroxidase epitope. *J Biol Chem* 2001; 276:28058–28067.
  62. Both P, Sobczak L, Breton C, Hann S, Nöbauer K, Paschinger K, Kozmon S, Mucha J, Wilson IB. Distantly related plant and nematode core  $\alpha$ 1,3-fucosyltransferases display similar trends in structure-function relationships. *Glycobiology* 2011; 21:1401–1415.
  63. Srikrishna G, Toomre DK, Manzi A, Panneerselvam K, Freeze HH, Varki A, Varki NM. A novel anionic modification of N-glycans on mammalian endothelial cells is recognized by activated neutrophils and modulates acute inflammatory responses. *J Immunol* 2001; 166:624–632.
  64. Chapman DA, Killian GJ. Glycosidase activities in principal cells, basal cells, fibroblasts and spermatozoa isolated from the rat epididymis. *Biol Reprod* 1984; 31:627–636.
  65. Fujihara Y, Tokuhira K, Muro Y, Kondoh G, Araki Y, Ikawa M, Okabe M. Expression of TEX101, regulated by ACE, is essential for the production of fertile mouse spermatozoa. *Proc Natl Acad Sci USA* 2013; 110:8111–8116.